Journal of Molecular Structure 1248 (2022) 131462

Contents lists available at ScienceDirect

Journal of Molecular Structure

journal homepage: www.elsevier.com/locate/molstr

Dielectric absorption correlated to ferromagnetic behavior in (Cr, Ni)-codoped 4H–SiC for microwave applications

B. Merabet[a], Ahmed J.H. Almaliky[b], A.H. Reshak[c,d,e,*], Muhammad M. Ramli[e], J. Bila[d]

[a] Faculty of Sciences and technology, Mustapha Stambouli University, Mascara 29000, Algeria
[b] Physics Department, Education College for Pure Science, University of Basrah, Basrah, Iraq
[c] Physics Department, College of Science, University of Basrah, Basrah, Iraq
[d] Department of Instrumentation and Control Engineering, Faculty of Mechanical Engineering, Czech Technical University in Prague, Technicka 4, Prague 6 166 07, Czech Republic
[e] Center of Excellence Geopolymer and Green Technology (CEGeoGTech), University Malaysia Perlis, 01007 Kangar, Perlis, Malaysia

ARTICLE INFO

Article history:
Received 20 June 2021
Revised 30 August 2021
Accepted 6 September 2021
Available online 11 September 2021

Keywords:
(NiCr)-codoped 4H–SiC
Microwaves absorbers
Ni coatings
Dielectric absorption
Ferromagnetic order

ABSTRACT

For (Cr, Ni)-codoped 4*H* silicon carbide SiC, electronic/optical properties are calculated, and a ferromagnetic (FM) order is detected. Doping Ni at Si sites should not destroy the effective coupling of the spins induced by Cr, could enormously boost the quality of absorbing electromagnetic waves, and acts as resist coatings for Cr-doped 4*H*-SiC. The metallic character shown by (Ni, Cr)-codoped 4H–SiC allow us using it in microwave circuits. Its FM order is mainly due to Cr impurities, so that the strong FM coupling originates from p-d hybridization interaction. Our results show that substituting Al for Ni either in (Al, Cr) or (Al, Cr)-doped 4H-SiC may improve the magnetism of 4H–SiCand enhance its microwave absorbing properties in the mm-wave band.

1. Introduction

Microwave (MW) circuits and wireless telecoms are rapidly developing, [1–6] while humans are more concerned with electromagnetic wave (EMW) pollution that has attracted extensive attention, due to undesirable effects on human life, biological health and precise instrument [7–12]. For instance, magnetic nanomaterials as EMW absorbers (EMWAs), can really delays EM pollution and strengthen defense capabilities of weapon systems [13–18]. To avoid EMW pollution caused by electronic and telecom systems, Cr-doped 4H–SiC are used, where Cr behaves as donor or acceptor and the dielectric properties of SiC can be changed through *n*- or *p*-type doping in the MW range, and enhanced dielectric loss and improved EM matching (beneficial to get excellent MW absorption performance) could be obtained [19]. Emerging EMWAs should exhibit thin matching thickness, lightweight, broad absorbing bandwidth, and strong EM absorption [20]. EMWAs become important, and absorption was the interest in MW absorbing materials, especially those suitable for high frequency (Ku-band, 12.4-18 GHz) absorption, is on the rise due to a rapid progress in radar systems and military aircraft [21–25]. Absorbers require wide frequency range, zero external magnetic field, thin absorption layer, that limit ferromagnetic (FM) materials to be applied in the MW frequency range above a few GHz, so that ferrites in the hexagonal crystal structure cause the FM resonance shifting towards lower frequency [26]. In EMWAs, the FM particles both reduce impedance mismatch at the front interface of the absorber, and increase absorption of EMWs [27]. One of the promising MW absorbent is silicon carbide (SiC); It owns wide waveband, strong absorption and thinness, shows good thermal stability and excellent mechanical strength at elevated temperature [28]. But unfortunately, SiC suffers from poor dielectric/magnetic properties and low conductivity that enormously limit its applications [29]. Practically, magnetic moments (MMs) in 4H-SiC may be obtained by doping this compound in the process of crystal growth, and implantation-induced lattice disorder and expansion may trigger the formation of high-spin SiC-transition metal (TM) systems [30]. Take for instance, Cr^{4+} ions used to overcome the handicap of SiC produce a spin ground state with a narrow, spectrally isolated, spin-selective, near-telecom optical interface [31]. Furthermore, in systems like Cr_2O_3–Al_2O_3–SiO_2, where substituting Al^{3+} by Cr^{3+} ions is preferential, octahedral positions as Cr^{3+} is likely to substitute Al^{3+} in such crystal [32]. However, Cr^{4+} ions in SiC and d^2 configuration in strong tetrahedral ligand field, are promising for integrated optics of interest for in-fiber long distance quantum communication, [33] and have the more stable configuration Cr^{+4} ions in monodoped 4H-SiC [34]. More-

* Corresponding author.
E-mail address: ali.reshak@uobasrah.edu.iq (A.H. Reshak).

https://doi.org/10.1016/j.molstruc.2021.131462
0022-2860/

over, Cr^{4+} are detected by placing devices into a photonic cavity to reduce the excited state lifetime by Purcell enhancement: large fraction of indistinguishable photons in near telecom zero-phonon lines would be further enhanced [35]. Hence, Cr-based absorbers areultrathin, broadband, and heat-tolerant, and perfectly absorb EMW and visible light, since Cr of high T_M of 1907°C is inexpensive and easy to fabricate [36]. In turn, Al element is also used in doping 4H-SiC, but it helps only to stabilize the SiC crystal structure inherent to 4H, with no FM feature was observed in the pristine 4H-SiC [37]. Song *et al.* [38] synthesized (Al, Cr)-codoped 4H-SiC by solid-state reaction, reporting no obvious role of Al element to modulate the carrier in SiC, but a FM order that weakens with increasing Cr content. Bai *et al.* [39] reported Co-based composites with impedance matching, and dielectric loss/ geometrical effect of great potential in developing lightweight and high-efficiency EMWAs, and described Fe/Mn-based composites with small reflection loss, large effective bandwidth, thin thickness, low density and good chemical stability as promising candidates for EMWAs [40].

Motivated by their work suggestions to explore new EMWAs, we intend here to overcame the above shortcoming through the (Cr, Ni) codoping strategy of 4H-SiC, to boost the FM order of Cr-doped 4H-SiC, and wear a resistance coating with nickel (Ni) used as protective surface layers against oxidation and corrosion [41]. In addition, Lin *et al.* [42] have reported no spin-polarization that Al can induce in (Ni, Al) codoped 4H-SiC, and even the FM exchange interaction is reduced due to the (Ni,Al) co-doping. Since Niis used in self-lubricating Si/SiC composites and enhances their tribological properties [43] it can be selected as the toughening phase in coating EMWAs. Improving magnetic/dielectric properties of materials is still very limited [44], and a systematic investigation of Cr–Ni–Si coatings for Cr-doped 4H-SiC based EMWAs (to limit EMW pollution) is needed. Although experiment plays a key role in testing EMWAs theory and provides the basis of their scientific knowledge, *theory is the essence of facts, and without theory scientific knowledge would be only worthy of the madhouse* (Olivier Heaviside). Besides belonging to the SiC series, 4H–SiC is of great interest, and its physical features, namely high thermal conductivity thermal stability, and chemical inertness, of SiC DMSs are excellent [45]. Although epitaxial 4H-SiC grown by Ito *et al.* [46] and Miyazawa *et al.* [47] by vertical hot-wall chemical vapor deposition reactor by employing an $H_2 + SiH_4 + C_3H_8$ or an $H_2 + SiH_4 + C_3H_8 + HCl$ gas system, until the present time (Cr, Ni)-codoped 4H–SiC are not synthesized yet, and not predicted except by the present study. In this paper, we present *ab initio* calculations results of Cr-doped and (Cr, Ni) codoped 4*H*-SiC, using accurate FP-LAPW calculations and performing a structural relaxation of the SiC lattice with substitutional Cr/Ni impurities. The results of densities of states (DOS)/electronic band structures (EBS), dielectric properties and magnetic ordering [48], allow predict that codoping 4*H*-SiC with Cr/Ni impurities can improve the MW performances for EMWAs, by suggesting all magnetic impurities alternatives in the wide bandgap (E_g) SiC semiconductor host, and obtaining metallic compounds.

2. Methodology and computational details

The crystal lattice of 4H–SiC can be represented by a sequence of hexagonal close-packed silicon-carbon bilayers. DFT band structure calculation [49] for bulk crystalline Cr/Ni-doped SiC and (Ni, Cr)-codoped SiC alloys is carried out within the Wien2K code, implementing the FP-LAPW [50] and GGA-PBE approximations [51] full relativistic effects are calculated with the Dirac equations for core states, and the scalar relativistic approximation is used for the other states [52]. The spin-orbit coupling is ignored here since it has a slight effect. Our DFT calculations are performed by using the highly accurate full-potential projector augmented wave method [53] whose potentials are used to describe electron–ion interactions representing ionic cores. The orbitals of ^{52}Cr: $3d^54s^1$; ^{58}Ni: $3d^84s^2$; ^{28}Si: $3s^23p^2$; ^{12}C: $2s^22p^2$ are treated as valence electrons. Brillouin zone (BZ) integrations are performed with the tetrahedron method in a Monkhorst–Pack *k* point mesh centered at high symmetry point Γ, inside the BZ [54]. To investigate the (Cr, Ni) effects on dielectric and magnetic properties of Cr-doped 4H–SiC and (Ni, Cr)-codoped 4H–SiC alloys (Fig. 1), Cr and Ni atoms substitute on the Si sites in a 72-atom supercell, corresponding to 3 × 3 × 1 supercell. Ni/Cr atoms replacing Si ones in such supercell are assessed for a common doping concentration of 2.78 %, [42,43] to avoid weak ferromagnetism order and magnetization decrease with increase in Ni/Cr concentrations [38]. We adopted a hexagonal $P6_3mc$ structure with 72 atoms in a primitive unit cell, and an FM phase with Ni and Cr both spin polarized. The unit cell is divided into non-overlapping muffin-tin (MT) spheres around the atomic sites and an interstitial region. The MT radii (R_{MT}) were taken to be 2.4, 2.45, 2.3 Bohr for (Cr, Ni), C and Si atoms, respectively. The $R_{MT} \times k_{MAX}$ parameter and separation energy between valence and core states are set to8 and −8Ry, respectively. The lattice parameters *a* and *c* of 4H-SiC in the $P6_3mc$ structure are taken to be3.081 and 10.096 Å, respectively [55]. The unit cell crystal structure of (Ni, Cr)-codoped 4H–SiCis generated from a 3D visualization program package (XCrySDen) [56]. Wyckoff sites of Si/C atoms in 4H-SiC system are such as Si or C atoms are respectively positioned in the 2a and 2b sites, and their atomic coordinates (*x, y, z*) were taken to be as follows: Si_1 (0, 0, 0.1875); Si_2 (1/3, 2/3, 0.4375); C_1 (0, 0, 0) and C_2 (1/3,2/3, 0.2599) [57]. However, Ni/Cr atoms in the codoped 4H–SiCoccupy optimized positions at Si sites.

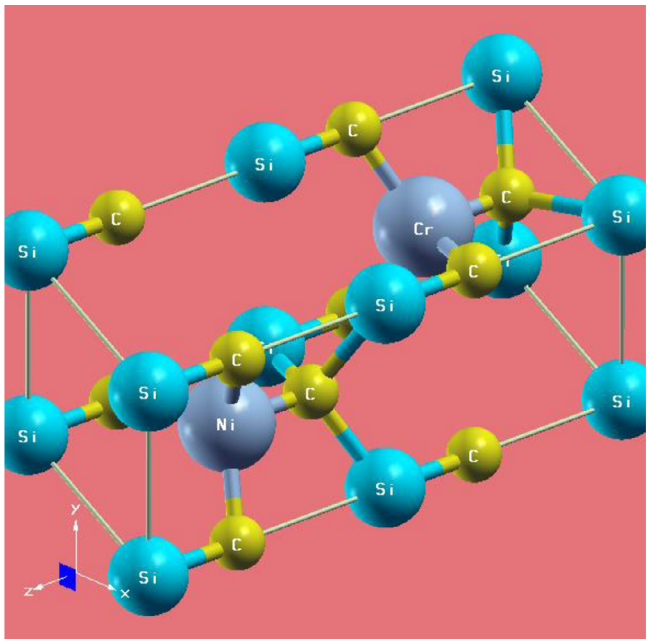

Fig. 1. Optimized (Cr, Ni)-codoped 4H-SiC primitive cell, with initial Wyckoff positions of Si/C atoms are: Si_1 (0,0,0.1875); Si_2 (1/3,2/3,0.4375); C_1 (0,0,0) and C_2 (1/3,2/3,0.2599), and hexagonal symmetry (#$P6_3mc$). Ni/Cr atoms are localized at C sites. Under full structural relaxation, the 72 atoms supercell structure was calculated to take into account changes in lattice parameters and internal atomic positions after substitution $(Ni_1,Cr_1)C_{34}Si_{36}$.

3. Results and discussions

4H–SiC (#$P6_3mc$) as a null MM material with indirect E_g of 2.25 eV, has a conduction band (CB) mainly contributed by Si-3p orbitals, however the valence band (VB) is specially occupied

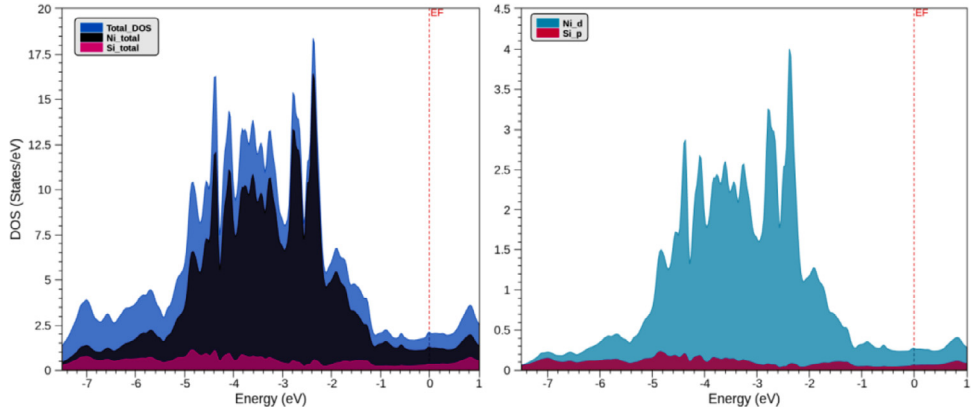

Fig. 2. Total and partial DOSs of NiSi : At $E_g \sim 2.25$ eV, $M_{TM}=0\mu_B$.

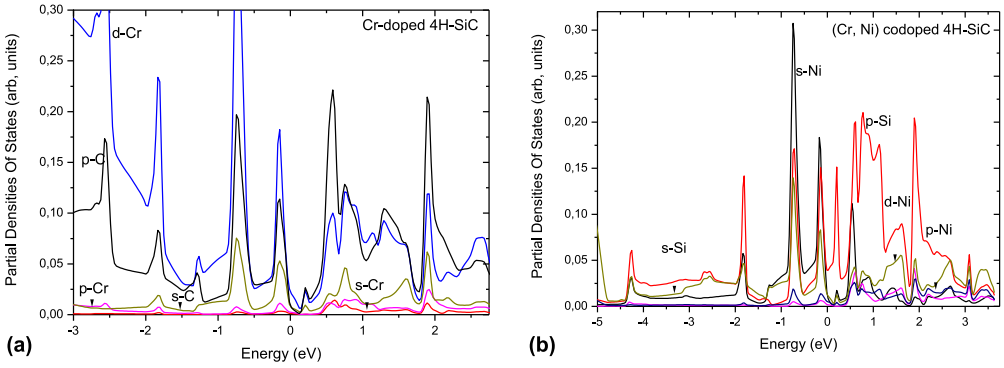

Fig. 3. DOSs of *a*) Cr-doped, *b*) (Cr, Ni)-codoped 4H-SiC systems.

by C-2p and Si-3p orbitals [57]. It has been experimentally reported that C/C composites in 4H–SiCshow high oxidative degradation and poor wear resistance at high temperature during exposure to an oxidizing atmosphere. Although EMW absorbing materials rely in experiment on doping amount, particle size and morphology, filling ratio and effective bandwidth, [58] nothing but theory is used to evaluate the EMW absorption ability (as in wormlike SiC nanowires in X-band) [59]. Let us focus on doping SiC by TM ions. Cr atoms in Cr-doped 4H–SiCbehave as donor impurities, and the mechanism of bonding Cr with Si atoms is so that neutral Cr electrons become involved in forming tetrahedral bonds with neighboring Si atoms [60]. However, it can also behave as an acceptor depending on its charge states, forms impurity levels in the gap of SiC, acting as deep-level double acceptor impurities [61]. In turn, Ni-coated SiC can solve issues of facile oxidation and magnetic aggregation, while improving the conductivity of SiC can enhance its dielectric properties [62]. Since SiC is mainly used for absorption of millimeter (mm) and centimeter (cm) waves, the 1mm wavelength (accordingly to ~1.24 meV energy) is chosen here to study all dielectric parameters of the three compounds.

On the one hand, we introduce here metallic and all non-FM systems NiSi compounds, [63] aiming to precipitate their probable growth on 4H–SiC. As Fig. 2 focusing on total and partial DOSs of NiSi can show, Ni d-DOS maximum is shifted from the Fermi level (E_F), so as its distribution can occupy two energy ranges: a first one poorly recovered with Si p-states, where d(Ni) max becomes poor from p(Si) states, hence a d–p resonance, and a second region taking part in d(Ni)–p(Si) hybridization, where p(Si) states make a greater contribution near E_F.NiSi studied for its unusual magnetic and thermodynamic properties like magnetic susceptibility and insulator-MT with increasing temperature, is described as a strongly correlated system, a possible Kondo insulator [64].

Fig. 2(*a,b*) show partial DOSs of Cr-doped and (Cr, Ni)-codoped 4H-SiC systems, where a strong hybridization between Cr:3d/C:2p orbitals exists. It is worth to be noticed that the mentioned powerful FM coupling should originate from p-d hybridization interaction, CB and VB are mainly contributed by Si-3p and (C-2p, Si-3p) orbitals respectively, and the metallic character subsists. Fig. 2(*b*) shows only majority-spin DOSs of (Cr, Ni)-codping in 4H–SiC,wereadjacent C spin polarized and FM coupling with Ni/Cr, due to the strong hybridization of Ni and Cr dopants with adjacent C atoms. The hybridized Ni: 3d-C: 2p-Cr: 3d chain formed through p-d coupling is responsible for the long-range FM coupling. Here, it is worth mentioning that the FM order do not originate from Ni but Cr atoms, since no significant change is mentioned in total MMs (remaining ~ 1.98 μB) after inducing Ni atoms.

On the other hand, and unlike (Al, Cr)-codoped 4H–SiC, where the key role of Al doping is to stabilize the crystal structure as -single-phase, and the magnetic characters is ascribed to be induced by the Cr element, [65] Ni codoping may not affect the magnetic properties, inducing weak FM order, the magnetization (Ni, Cr)-codoped SiC is mainly due to the Cr impurity [39]. In the (Ni, Cr)-codoped SiC system, and its FM order can be attributed to the strong p-d hybridization interaction between Ni and Cr atoms and their closest neighbor C atoms. For (Ni, Cr)-codoped SiC systems, the ground state should be a FM coupling between Ni and Cr atoms [66]. The CB is mainly contributed by Si-3p orbitals and the valence band (VB) is mainly contributed by C-2p and Si-3p orbitals and pure SiC material is nonmagnetic [67]. To investigate the electronic properties of Cr/Ni-doped SiC and (Cr, Ni)-codoped SiC in deep, we also calculated their EBSs, as shown in Figs. 4(*a,b*) and 5, respectively. The incorporated TMs in group IV compounds (SiC here) are usually spin-polarized, and local spins on these TMs can couple with each other via hole mediated or double exchange

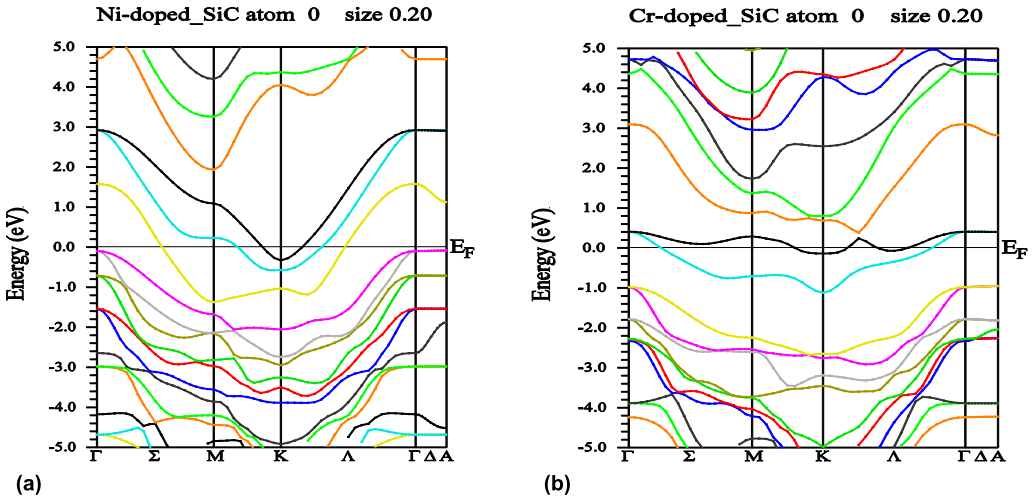

Fig. 4. Band structure of *a*) Cr- *b*) Ni-doped 4H-SiC systems.

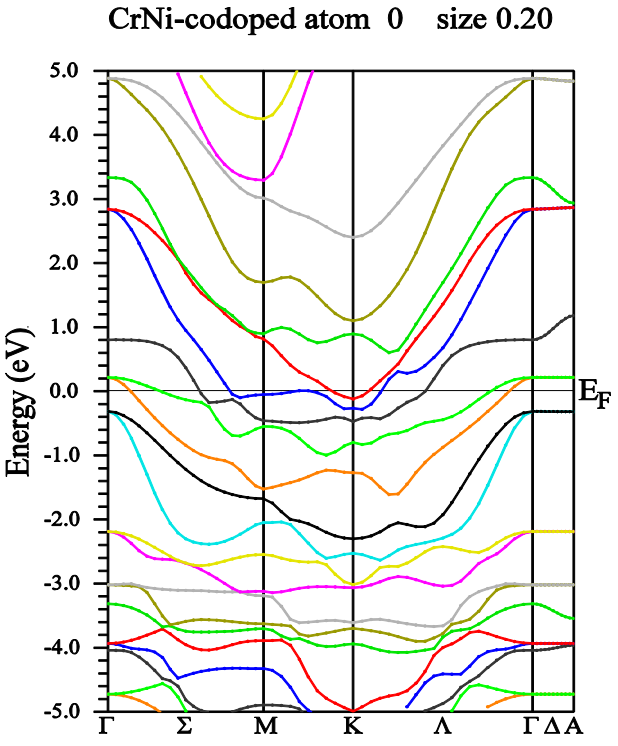

Fig. 5. Band structure of the (Cr, Ni)-codoped 4H-SiC system.

mechanisms. Since Cr is mostly acceptor, its acceptor levels are either close to the condition band(CB) maximum or deep in the gap. Hence, Cr-doping in SiC cannot induce holes, excluding the hole mediated set apart coupling, while the local spins can still coupled through double exchange. For the (Cr, Ni)-codoped SiC system mainly (Fig. 7), no gap appears, while CBs crosses E_F, overlapping with each other and proving the metallic character of this system.

The second part of our calculations were performed on optical properties of the three systems: Cr/Ni-doped SiC and (Cr, Ni)-codoped SiC, aiming to reduce the reflection coefficient of the interface of the proposed EMWAs, where impedance matching material/free space is required. MW absorption properties of EMWAs are obtained via relative complex permittivities ε and permeabilities μ, appearing as important parameters from strong applications of FM metals as EMWAs [67]. In terms of impedance (η) and propagation constant (γ) for EM absorbers, the permittivity (ε) and permeability (μ) of materials, as functions of the angular frequency ω, are given by $\varepsilon = \frac{\gamma}{j\omega\eta}$ and $\mu = \frac{j\eta}{j\omega}$ [68], and Kramers-Kronig (KK) relations are formulated mainly for EM excitation [69]. For impedance matching requirements, the impedance $\eta = \sqrt{\mu/\varepsilon}$ of EMWAs is so that the reflection of incident wave is minimized: dielectric and/or magnetic losses must be high to achieve better EM absorption performance [70]. Real and imaginary parts of ε are also connected by KK relations, used in nonlinear optics to calculate refractive indexes $n = \sqrt{\varepsilon_1 + i\varepsilon_2}$ of materials by measuring absorbance, and check self-consistency of experiment or model-generated data [71]. EMWs must be absorbed while energy should be transformed into heat, which requires high dielectric/magnetic losses that are determined by the complex permittivity and permeability, given as $\varepsilon_r = \varepsilon' + i\varepsilon''$ and $\mu_r = \mu' + i\mu''$ [70]. For all of our systems both parts of ε are shown in Figs. 6 and 7. The calculated complex dielectric constants of our systems at 300 GHz are found to be 179.1+*i*24.5,193.1+ *i*21.6, and 109.7 + *i*13.4 for Ni-doped SiC, Cr-doped SiC and (Cr, Ni)-codoped SiC, respectively.

It is clearly seen that the real part of ε of the Ni-doped 4H-SiC is less than those of Cr-doped SiC and (Cr, Ni)-codoped SiC, and imaginary part of ε of Ni-doped SiC is bigger than that of (Cr, Ni)-codoped SiC but less than that of Cr-doped SiC. Both parts of ε for all systems show up trends at the wavelength of 1mm,that may be explained by an increased lagging near the polarization response on the electric-filed change [72]. Due to probable μ/ε mismatching at interface, proportional increasing of μ can compensate the reflection coefficient of the interface by the impedance matching material and free space. ε' and ε'' of MM-based SiC composites, usually increase dramatically compared with those of SiC, [70] and with no magnetic losses ($\mu' \sim 0$ and $\mu'' \sim 1$).It is worth mentioning that mm waves (≤300 GHz), applied to radar, microwave WiFi, high-performance5G, [73] radio astronomy, security screening, remote sensing, imaging, automotive radars, [74–77] may involve our systems as promising candidates. For different microwave absorption bands (application at different frequencies) suitable thicknesses for EMWAs should be adjusted [78]. An appropriate (Cr, Ni) codoping in SiC can increase its dielectric loss, enhance the impedance matching to facilitate incident microwaves entering such composites, therefore improve their performances for microwave absorption. MW-absorbing property of SiC can be enhanced by dispersing ceramic matrix with (Cr, Ni) FM-EMWAs. Ni coating on Cr-doped SiC can effectively improve absorbing properties of SiC. The calculated absorption coefficients (α) are so as that of the Ni-doped 4H-SiC is bigger than those of Cr-doped 4H-

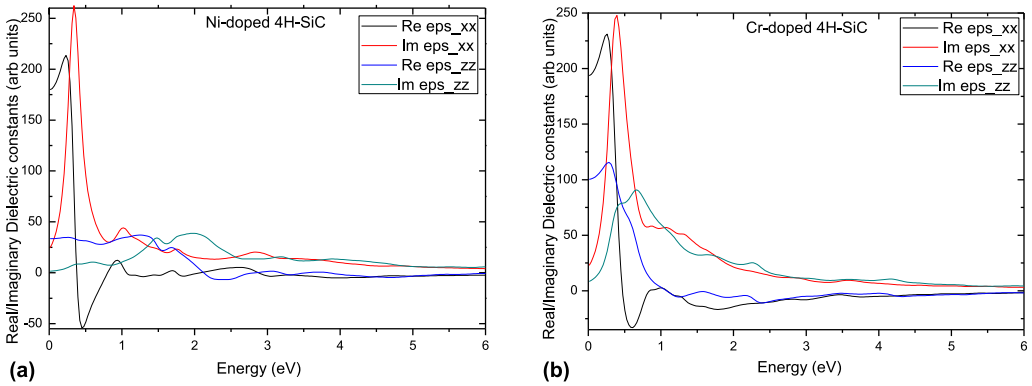

Fig. 6. Real and imaginary parts of ε for *a*) Ni-doped SiC system. At 1.24∼meV (300Ghz), ε =179.1+*i*24.5; $\alpha\sim$ 0.126 cm^{-1}; Real part of (n) ∼13.4. *b*) Cr-doped 4H-SiC system; ε =193.1+*i*21.6; $\alpha\sim$ 0.11 cm^{-1}; R(n) = 13.9.

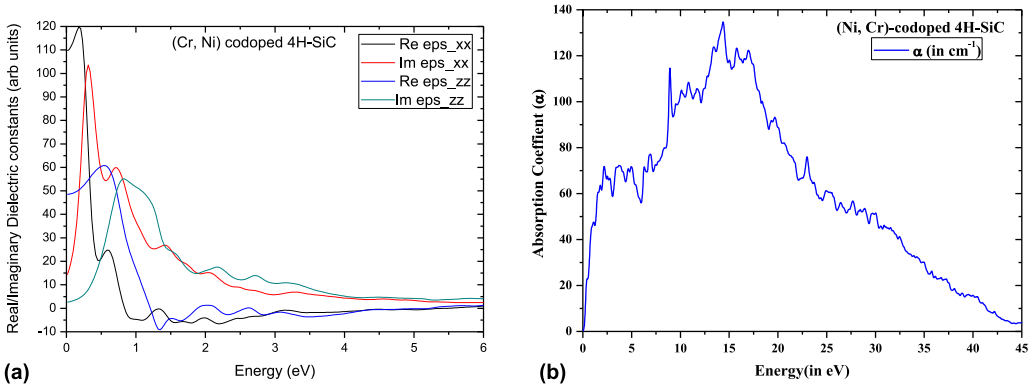

Fig. 7. *a*) Real and imaginary parts of the dielectric function *b*) Absorption coefficient of (Cr, Ni)-codoped SiC, with : ε = 109.7 + *i* 13; R(n)= 10.5, and α=0.094 cm^{-1}at ∼1.24 meV (300Ghz).

SiC and (Cr, Ni)-codoped SiC, and imaginary part of ε of Ni-doped SiC is bigger than that of (Cr, Ni)-codoped SiC but less that of Cr-doped SiC. For comparison purposes, Kuang *et al.* [79] reported experimentally that dielectric properties (in the 8.2–12.4 GHz range) of $Ni_xSi_{1-x}C$ are slightly higher than those of undoped SiC for x = 05%, however by increasing the doping to x = 1%, the dielectric properties were boosted as follows: dielectric loss from1.75 to 1.99, and ε from 8.13 to 8.53. Majid *et al.* [80] verified theoretically that in 8.2–12.4 GHz range, but reported via X-rays analysis that with increasing Ni a shrink in SiC lattice is caused. Moreover, for Cr doping in SiC ($Cr_xSi_{1-x}C$), Lu *et al.* [81] reported that in that frequency range, ε of SiC was slightly improved after doping Cr, but the effect is not as remarkable as Al doping, ε = 75.593 + *i* 24.515. Our results are comparable with those mentioned above, provided that the chosen 300Ghz frequency is lower compared to the 8.2–12.4 GHz range. The real ε of Cr-doped SiC is slightly higher than that of Ni-doped SiC, but inversely for the imaginary parts. The undoped SiC compound remains with the lowest ε of 5.10 [79]. Although (Ni, Cr) codoping decreases slightly ε of SiC, this appears significantly much better than that of SiC undoped. It is clear that by optimizing the doping amount of Cr/Ni TMs, the MW absorption ability of the undoped SiC compound has been effectively improved, due to enhancement in ε.

As well known, the relationship between the refractive index and reflectivity has practical significance in that it may allow estimating the severity of clear air turbulence from MW devices reflectivity. Moreover, highest refractive indexes as a negative feature in MW devices, raise significantly absorption losses and could be beneficial for EMWAs. Orders of magnitude of such indexes (at ∼1.24 meV) are given in captions of Figs. 6 and 7.*a*, showing a higher value of 13.9for the Cr doped system, compared to those of Ni-SiC and (Ni, Cr)-SiC found to be 13.4 and 10.5 respectively, may allow it when codoping Ni-SiC to be a good candidate for EMWAs. Fig.7.*b* shows a weak α for (Ni,Cr)-SiC that may convert EMWs into heat, and these must be attenuated. Our results suggest that though a compromise between Cr and Ni-performances doping SiC separately, (Ni, Cr)-SiC coated with Ni should exhibit better features as a good candidate for mm-waves applications. It has been shown that adding small amounts of Cr and Ni in SiC can affect the dielectric and magnetic losses, and enhance microwave absorption performances of the (Cr,Ni)-SiC composite.

4. Summary

We have calculated electronic/optical structures of (Ni/Cr)-doped SiC systems separately, by using the accurate ab initio FP-LAPW technique. The results show a more favorable FM state in the (Cr, Ni/Cr)-based systems, that originates from a strong p-d hybridization interaction between Cr and nearest C neighbors(3d-C/2p-Cr), giving rise to enhanced dipole polarization intensities and electronic polarizations, while the Ni-based system is NM. This can provide a new route for potential applications of (Cr,Ni)-codoped SiC system in MW devices. Dielectric and magnetic properties of Cr-doping in SiC should be boosted by adding Ni dopant (coating) for success in enriching such properties. (Cr,Ni)-codoping in SiC is be predicted to be applied as an excellent EMWA, with good thermal stability, excellent mechanical strength at elevated temperature, lightweight, special dielectric and electrical properties, and many practical and potential applications. (Cr, Ni)-SiC system can overcome SiC shortcomings, such as poor dielectric properties resulting from single polarization, low conductivity and poor

magnetic properties. Such doping approach shed light on synthesizing EMWAs with strong dielectric attenuation performance.

Declaration of Competing Interest

The authors declare that they have no known competing financial interests or personal relationships that could have appeared to influence the work reported in this paper.

References

[1] J.P. Barham, E. Koyama, Y. Norikane, N. Ohneda, T. Yoshimura, The Chemical Society of Japan & Wiley(Wiley Online Library), Chem. Rec. 18 (2018) 1–17.
[2] M. Makimoto and S. Yamashita, Microwave Resonators and Filters for Wireless Communication Theory, Design and Application, Springer 2001, Volume 4. ISBN : 978-3-642-08700-4.
[3] A. Doumounia, M. Gosset, F. Cazenave, M. Kacou, F. Zougmore, Rainfall monitoring based on microwave links from cellular telecommunication networks: first results from a West African test bed, Am. Geophys. Union (GeophysicalResearchLetters) (2014), doi:10.1002/2014GL060724.
[4] T. Nagatsuma, G. Ducournau, C. Renaud, Advances in terahertz communications accelerated by photonics, Nat. Photon 10 (2016) 371–379, doi:10.1038/nphoton.2016.65.
[5] S Horikoshi, RF Schiffmann, J Fukushima, N Serpone, Microwave chemical and materials processing, Springer (2018) ISBN978-981-10-6466-1.
[6] Y. Okano, S. Ogino, K. Ishikawa, IEEE Trans. Microwave Theory Tech. 60 (8) (2012) 2456–2464, doi:10.1109/TMTT.2012.2202680.
[7] M. Zhang, Z. Lia, T. Wang, S. Ding, G. Song, J. Zhao, A. Meng, H. Yu, Q. Li, Chem. Eng. J. 362 (2019) 619–627.
[8] M. Tonouchi, Cutting-edge terahertz technology, Nat. Photonics 1 (2007) 97–105.
[9] P.D. Inskip, R.E. Tarone, E.E. Hatch, T.C. Wilcosky, W.R. Shapiro, R.G. Selker, H.A. Fine, P.M. Black, J.S. Loeffler, M.S. Linet, New Engl. J. Med. 344 (2001) 79–86.
[10] J. Wiart, A. Hadjem, M.F. Wong, I. Bloch, Phys. Med. Biol. 53 (2008) 3681–3695.
[11] T. Wang, H.D. Wang, X. Chi, R. Li, J.B. Wang, Carbon 7 (2014) 312–318.
[12] D.P. Sun, Q. Zou, G.Q. Qian, C. Sun, W. Jiang, F.S. Li, Acta Mater. 61 (2013) 5829–5834.
[13] L. Liu, N. He, J. Sun, P. Hu, R. He, J. Cheng, W. Tian, G. Tong, Progr. Natl. Sci. (2018), doi:10.1016/j.pnsc.2018.08.008.
[14] Y.H. Chen, Z.H. Huang, M.M. Lu, W.Q. Cao, J. Yuan, D.Q. Zhang, M.S. Cao, J. Mater. Chem. A 3 (2015) 12621–12625.
[15] C.L. Zhu, M.L. Zhang, Y.J. Qiao, G. Xiao, F. Zhang, Y.J. Chen, J. Phys. Chem. C 114 (2010) 16229–16235.
[16] W.Q. Cao, X.X. Wang, J. Yuan, W.Z. Wang, M.S. Cao, J. Mater. Chem. C 3 (2015) 10017–10022.
[17] R.C. Che, L.M. Peng, X.F. Duan, Q. Chen, X.L. Liang, Adv. Mater. 16 (2004) 401–405.
[18] B. Wen, M.S. Cao, M.M. Lu, W.Q. Cao, H.L. Shi, J. Liu, X.X. Wang, H.B. Jin, X.Y. Fang, W.Z. Wang, J. Yuan, Adv. Mater. 26 (2014) 3484–3489.
[19] JF Justo, WVM Machado, LVC. Assali, Physica B 378 (2006) 376.
[20] Z. Jia, Di D. Lan, K. Lin, M. Qin, K. Kou, G. Wu, H. Wu, J. Mater. Sci. Mater. Electron. 29 (2018) pages 17122–17136.
[21] P.J. Bora, S.M. Harstad, S. Gupta, V.K. Pecharsky, K.J. Vinoy, P.C. Ramamurthy, R.L. Hadimani, Mater. Res. Express 6 (2019) 055053.
[22] X.G. Liu, B. Li, D.Y. Geng, W.B. Cui, F. Yang, Z.G. Xie, D.J. Kang, Z.D. Zhang, Carbon N. Y., 47 (2009) 470–474.
[23] F. Qin, H.X. Peng, Prog. Mater. Sci. 58 (2013) 183–259.
[24] P.J. Bora, M. Porwal, K.J. Vinoy, Kishore, P.C. Ramamurthy, G. Madras, Compos. Part B Eng. 134 (2018) 151–163.
[25] K.J. Vinoy, R.M. Jha, Sadhana, 20 (1995) 815–850 B. Zhao, X. Guo, Y. Zhou, T. Su, C. Ma and R. Zhang, CrystEngComm, 2017, 19, 2178–2186.
[26] Liu L. Chao, Anjali A. Sharma, M.N. Afsar, Microwave and millimeter wave ferromagnetic absorption of nanoferrites, IEEE Trans. Magn. 48 (11) (2012) pp2773-2776, doi:10.1109/TMAG.2012.2200666.
[27] V.B. Bregar, IEEE Trans. Magn. 40 (2004) 3.
[28] P. Wang, L. Cheng, L. Zhang, Chem. Eng. J. 338 (2018) 248–260.
[29] C. Liang, Z. Wang, Chem. Eng. J. 373 (2019) 598–605.
[30] A.V. Los, A.N. Timoshevskii, V.F. Los, S.A. Kalkuta, Phys. Rev. B 76 (2007) 165204.
[31] B. Diler, S.J. Whiteley, C.P. Anderson, et al., npj Quantum Inf. 6 (2020) 11.
[32] Aladesuyi A. Olanrewaju, et al., IOP Conf. Ser.: Mater. Sci. Eng. 509 (2019) 012007.
[33] B. Diler, S.J. Whiteley, C.P. Anderson, G. Wolfowicz, M.E. Wesson, E.S. Bielejec, F.J. Heremans, D.D. Awschalom, Coherent control and high-fidelity readout of chromium ions in commercial silicon carbide, Npj Quantum Inf. 6 (1) (2020), doi:10.1038/s41534-020-0247-7.
[34] Tong T. Liang, Ruixin R. Chen, Shunwei S. Xu, First principles calculations on magnetic and optical properties of (Cr, Mn) co-doped 4H-SiC, Mol. Phys. 119 (2021) 14, doi:10.1080/00268976.2021.1953171.
[35] A.M. Dibos, et al., Phys. Rev. Lett. 120 (2018) 243601.
[36] I. Kima, S. Soa, A.S. Rana, M.Q. Mehmood, J. Rho, Nanophotonics 7 (11) (2018) 1827–1833.
[37] Bo Song, H. Bao, H. Li, M. Lei, T. Peng, J. Jian, J. Liu, W. Wang, W. Wang, X. Chen, J. Am. Chem. Soc. 131 (2009) 1376–1377.
[38] B. Song, X.L. Chen, J.C. Han, G. Wang, H.Q. Bao, L.B. Duan, K.X. Zhu, H. Li, Z.H. Zhang, W.Y. Wang, W.J. Wang, X.H Zhang, S.H. Meng, Raman scattering and magnetizations studies of (Al, Cr)-codoped 4H-SiC, J. Magn. Magn. Mater. 323 (22) (2011) 2876–2882, doi:10.1016/j.jmmm.2011.06.044.
[39] YiY.-Wen W. Bai, Guimei G. Shi, Jun J. Gao, Fa-Nian Shi, MOF decomposed for the preparation of Co_3O_4/N-doped carbon withexcellent microwave absorption, J. Solid State Chem. 288 (2020) 121401.
[40] YiY.-Wen W. Bai, Guimei G. Shi, Jun J. Gao, Fa-Nian Shi, Synthesis, crystal structure of a iron-manganese bimetal MOF and its graphene composites with enhanced microwave absorption properties, J. Phys. Chem. Solids 148 (2021) 109657.
[41] W.L. Cheng, Z.F. Zhou, P.W. Shum, K.Y. Li, Effect of Ni addition on the structure and properties of Cr–Ni–N coatings deposited by closed-field unbalanced magnetron sputtering ion plating, Surf. Coat. Technol. 229 (2013) 84–89 Cheng, W. L., Zhou, Z. F., Shum, P. W., & Li, K. Y., Surface and Coatings Technology, 229 (2013) 84–89, doi:10.1016/j.surfcoat.2012.12.032.
[42] L. Lin, J. Huang, W. Yu, H. Tao, L. Zhu, P. Wang, Z. Zhang, J. Zhang, Comput. Mater. Sci. 155 (2018) 169–174.
[43] M. Zhang, J. Huang, X. Liu, L. Lin, H. Tao, Electronic Structure and High Magnetic Properties of (Cr, Co)-codoped 4H–SiC Studied by First-Principle Calculations, Crystals 10 (2020) 634, doi:10.3390/cryst10080634.
[44] A.H. Reshak, Saleem S.Ayaz A. Khan, Thermoelectric properties, electronic structure and optoelectronic properties of anisotropic $Ba_2Tl_2CuO_6$ single crystal from DFT approach, J. Magn. Magn. Mater. 354 (2014) 216–221, doi:10.1016/j.jmmm.2013.11.014.
[45] B. Zhang, L. Zhu, L. Lin, W. Yu, H. Tao, Y. Xu, J. Huang, Electronic structures and ferromagnetism in (Fe,Cr)-codoped 4H–SiC from first-principles investigations, Vacuum (2019), doi:10.1016/j.vacuum.2019.05.03.
[46] M. Ito, L. Storasta, and H. Tsuchida, Appl. Phys. Express 1, 015001 (2008).
[47] T. Miyazawa, T. Tawara, H. Tsuchida, Mater. Sci. Forum 897 (2017) 51 Yang, A., Murata, K., Miyazawa, T., Tawara, T., Tsuchida, H. (2019). Analysis of carrier lifetimes in N^+B- doped n-type 4H-SiC epilayers. Journal of Applied Physics, 126(5), 055103. doi:10.1063/1.5097718.
[48] Chen C. Zichen, Li L. Hejun, Fu F. Qiangang, Surf. Coat. Technol. 213 (2012) 207–215.
[49] P. Hohenberg, W. Kohn, Phys. Rev. 136 (1964) B864 Kohn W and Sham L J 1965 Phys. Rev. 140 A1133.
[50] P. Blaha, K. Schwarz, G.K.H. Madsen, D. Kvasnicka, J. Luitz, An Augmented Plane Wave Plus Local OrbitalsProgram For Calculating Cryst Properties (Wien2k), ViennaUniv. Technol. Austria (2001) (ISBN 3-9501031-1-2).
[51] J.P. Perdew, K. Burke, M. Ernzerhof, Phys. Rev.Lett. 77 (1996) 3865.
[52] D. Singh, Plane Waves Pseudopotentials and theLAPW method, Kluwer Academic, Boston, 1994.
[53] E. Blochl, O. Jepsen, O.K. Andersen, Phys. Rev. B49 (1994) 16223.
[54] P.E. Blochl, Phys. Rev. B 50 (1994) 17953.
[55] B. Zhang, L. Zhu, L. Lin, W. Yu, H. Tao, Y. Xu, G. Fei Peng, L. Lixin, J. Huang, Vacuum (2019), doi:10.1016/j.vacuum.2019.05.039.
[56] A. Kokalj, XCrySDen—a new program for displaying crystalline structures and electron densities, J. Mol. Graph. Model. 17 (3–4) (1999) 176–179 IssuesJune–August.
[57] W. Li, L. Wang, L. Bian, F. Dong, M. Song, J. Shao, S. Jiang, H. Guo, AIP Adv. 9 (2019) 055007, doi:10.1063/1.5093576.
[58] Z. Zhao, K. Kou, H. Wu, 2-Methylimidazole-mediated hierarchical Co3O4/N-doped carbon/short-carbon-fiber composite as high-performance electromagnetic wave absorber, J. Colloid Interface Sci. (2020), doi:10.1016/j.jcis.2020.04.037.
[59] J. Kuang, T. Xiao, X. Hou, Q. Zheng, Q. Wang, P. Jiang, W. Cao, Microwave synthesis of worm-like SiC nanowires for thin electromagnetic wave absorbing materials, Ceram. Int. (2019), doi:10.1016/j.ceramint.2019.03.040.
[60] A. Zywietz, J. Furthmüller, F. Bechstedt, Phys. Rev. B 59 (1999) 15166– Published 15 June.
[61] V.Q. Bui, TanT.-Tien T. Pham, S. Hoai-Vu, Nguyen N. Hung, M. Le, J. Phys. Chem. C 117 (2013) 44 23364-23371.
[62] Zhi Z.Jie J. Li, Gui G.Mei M. Shi, Qian Q. Zhao, J. Mater. Sci.: Mater. Electron 28 (2017) 5887–5897, doi:10.1007/s10854-016-6262-y.
[63] D. Connetable, O. Thomas, J. Alloys Compd. 509 (2011) 2639–2644 Meyer_J. Alloys and Compounds 262-263 (1997) 235-237.
[64] P. Goel, M.K. Gupta, S.K. Mishra, B. Singh, R. Mittal, S.L. Chaplot, Front. Chem. 6 (2018), doi:10.3389/fchem.2018.00331.
[65] S. Bet, N. Quick, A. Kar, Acta Mater. 56 (8) (2008) 1857–1867.
[66] B. Zhang, L. Zhu, L. Lin, W. Yu, H. Tao, Y. Xu, J. Huang, Vacuum 167 (2019) 59–63.
[67] S.-S. Kim, S.-T. Kim, Y.-C. Yoon, K.-S. Lee, J. Appl. Phys. 97 (2005) 10F905.
[68] Vasundara V.V. Varadan, Ruyen R. Ro, Unique retrieval of complex permittivity and permeability of dispersive materials from reflection and transmitted fields by enforcing causality, IEEE Trans. Microwave Theory Tech. 55 (10) (2007) 2224–2230 October, K-Y. Park, S-E. Lee, C-G. Kim, J-H. Han, Fabrication and electromagnetic characteristics of electromagnetic wave absorbing sandwich structures, Composites Science and Technology 66 (2006) 576–584. doi:10.1016/j.compscitech.2005.05.034.
[69] C.M. Watts, X. Liu, W.J. Padilla, Metamaterial Electromagnetic Wave Absorbers, Adv. Mater. 24 (23) (2012) OP98–OP120, doi:10.1002/adma.201200674.

[70] C. Liu, D. Yu, D.W. Kirk, Y. Xu, Electromagnetic wave absorption of Silicon carbide based materials, R. Soc. Chem. (RSC) Adv., RSC Adv. 7 (2017) 595–605, doi:10.1039/C6RA25142K.
[71] V. Lucarini, J.J. Saarinen, K.-E. Peiponen, Multiple subtractive Kramers–Kronig relations for arbitrary-order harmonic generation susceptibilities, Opt. Commun. 218 (2003) 409–414.
[72] H. Wang, H. Guo, Y. Dai, D. Geng, Z. Han, D. Li, T. Yang, S. Ma, W. Liu, Z. Zhang, Appl. Phys. Lett. 101 (2012) 083116–083114.
[73] R.N. Kostoff, P. Herou, M. Aschner, A. Tsatsakis, Adverse health effects of 5G mobile networking technology under real-life conditions, Toxicol. Lett. 323 (2020) 35–40, doi:10.1016/j.toxlet.2020.01.020.
[74] V. Jain, F. Tzeng, L. Zhou, P. Heydari, A Single-Chip Dual-Band 22–29-GHz/77–81-GHz BiCMOS Transceiver for Automotive Radars, IEEE J. Solid-State Circuits 44 (12) (Dec. 2009) 3469–3485, doi:10.1109/JSSC.2009.2032583.
[75] K.B. Cooper, et al., G-Band radar for humidity and cloud remote sensing, IEEE Trans. Geosci. Remote Sens. 59 (2) (Feb. 2021) 1106–1117, doi:10.1109/TGRS.2020.2995325.
[76] E.R. Brown, Fundamentals of Terrestrial Millimeter-Wave and THz Remote Sensing, Int. J. High Speed Electron. Syst. 13 (04) (2003) 995–1097, doi:10.1142/S0129156403002125.
[77] R.N. Kostoff, P. Heroux, M. Aschner, A. Tsatsakis, Adverse health effects of 5G mobile networking technology under real-life conditions, Toxicol. Lett. 323 (2020) 35–40, doi:10.1016/j.toxlet.2020.01.020.
[78] S. Du, H. Chen, R. Hong, Preparation and electromagnetic properties characterization of reduced graphene oxide/strontium hexaferrite nanocomposites, De Gruyter Nanotechnol. Rev. 9 (2020) 105–114, doi:10.1515/ntrev-2020-0010.
[79] J. Kuang, T. Xiao, Q. Zheng, S. Xiong, Q. Wang, P. Jiang, W. Cao, Dielectric permittivity and microwave absorption properties of transition metal Ni and Mn doped SiC nanowires, Ceram. Int. (2020), doi:10.1016/j.ceramint.2020.02.069.
[80] A. Majid, N. Rani, M.F. Malik, N. Ahmad, Najam-al-Hassan, F. Hussain, A. Shakoor, A review on transition metal doped silicon carbide, Ceram. Int. (2019), doi:10.1016/j.ceramint.2019.01.
[81] X. Lu, T. Zhao, Q. Lei, X. Yan, J. Ren, P. La, Effects of co-doping on electronic structure and optical properties of 3C-SiC from first-principles method, Comput. Mater. Sci. 170 (2019) 109172, doi:10.1016/j.commatsci.2019.10.